Heliyon 10 (2024) e32466

Contents lists available at ScienceDirect

Heliyon

journal homepage: www.cell.com/heliyon

Research article

Sirtuin 5-driven meiotic spindle assembly and actin-based migration in mouse oocyte meiosis

Cong Ma [a,b,c,1], Xueke Zhang [a,b,c,1], Yingying Zhang [a], Hongzhen Ruan [a], Xiaofeng Xu [a], Caiyun Wu [a], Zhiming Ding [a,b,c,**], Yunxia Cao [a,b,c,d,e,f,g,*]

[a] *Reproductive Medicine Center, Department of Obstetrics and Gynecology, The First Affiliated Hospital of Anhui Medical University, No.218 Jixi Road, Hefei, 230022, China*

[b] *NHC Key Laboratory of Study on Abnormal Gametes and Reproductive Tract, Anhui Medical University, No.81 Meishan Road, Hefei, 230032, China*

[c] *Key Laboratory of Population Health Across Life Cycle, Anhui Medical University, Ministry of Education of the People's Republic of China, No.81 Meishan Road, Hefei, 230032, China*

[d] *Engineering Research Center of Biopreservation and Artificial Organs, Ministry of Education, No.81 Meishan Road, Hefei, 230032, Anhui, China*

[e] *Anhui Province Key Laboratory of Reproductive Health and Genetics, No.81 Meishan Road, Hefei, 230032, China*

[f] *Biopreservation and Artificial Organs, Anhui Provincial Engineering Research Center, Anhui Medical University, No.81 Meishan Road, Hefei, 230032, China*

[g] *Anhui Provincial Institute of Translational Medicine, No.81 Meishan Road, Hefei, 230032, China*

ARTICLE INFO

Keywords:
Sirtuin 5
Oocyte
Meosis
Spindle migration
F-actin

ABSTRACT

Sirtuin 5 (Sirt5), a member of the Sirtuin family, is involved in various intracellular biological processes. However, the function of Sirt5 in oocyte maturation has not been clearly elucidated. In this study, we observed that Sirt5 was persistently expressed during the meiotic division of mouse oocytes, with a notable decline in expression in aging oocytes. Sirt5 inhibition led to the failure of the first polar body extrusion and induced cell cycle arrest, indicative of unsuccessful oocyte maturation. Furthermore, Sirt5 inhibition was associated with the extrusion of abnormally large polar bodies, suggesting disrupted asymmetric oocyte division. Mechanistically, the inhibition of Sirt5 resulted in aberrant spindle assembly and disordered chromosome alignment in oocytes. Moreover, Sirt5 inhibition caused the spindle to be centrally located in the oocyte without migrating to the cortical region, consequently preventing the formation of the actin cap. Further investigation revealed that Sirt5 inhibition notably diminished the expression of phosphorylated cofilin and profilin1, while increasing cytoplasmic F-actin levels. These findings suggest that Sirt5 inhibition during oocyte maturation adversely affects spindle assembly and chromosome alignment and disrupts actin dynamics impairing spindle migration and contributing to the failure of symmetric oocyte division and maturation.

* Corresponding author. Reproductive Medicine Center, Department of Obstetrics and Gynecology, The First Affiliated Hospital of Anhui Medical University, No.218 Jixi Road, Hefei, 230022, China.

** Corresponding author. Reproductive Medicine Center, Department of Obstetrics and Gynecology, The First Affiliated Hospital of Anhui Medical University, No.218 Jixi Road, Hefei, 230022, China.

E-mail addresses: dingzhiming10@163.com (Z. Ding), caoyunxia5972@ahmu.edu.cn (Y. Cao).

[1] These authors contribute equally and should be considered as co-first authors.

https://doi.org/10.1016/j.heliyon.2024.e32466
Received 25 January 2024; Received in revised form 21 May 2024; Accepted 4 June 2024
Available online 5 June 2024

1. Introduction

Ovarian aging is characterized by a reduction in both the quantity and quality of oocytes [1]. Notably, oocytes from aged ovaries are more prone to meiotic errors, leading to a higher incidence of aneuploidy in eggs, which consequently results in embryonic aneuploidy and stunted embryonic developmental potential [2]. Unlike males, who have a continually renewing supply of spermatogonia, females have a finite ovarian reserve, which is susceptible to genetic mutations [3], endocrine disruptors [4], radiation therapy and chemotherapy [5]. Therefore, the production of high-quality oocytes capable of undergoing precise meiosis is of paramount importance for successful fertilization and subsequent embryonic development [6]. The accurate transmission of genetic information to the offspring through gametes necessitates precise chromosomal recombination and segregation during meiosis [7]. During fertilization, both the egg and the sperm should contribute precisely one copy of each chromosome to the embryo. However, oocyte meiosis is more prolonged and complex compared with spermatogenesis, and chromosomal segregation errors are more likely, leading to aneuploidy in the eggs. Substantial clinical data indicate that aneuploidy, primarily caused by aberrant oocyte meiosis, is a leading cause of infertility, miscarriages, and congenital defects [8–10]. However, the regulatory mechanisms involved in oocyte meiosis are not fully understood yet. Elucidating the regulatory mechanisms of oocyte meiosis and exploring potential molecular targets for modulating oocyte meiosis carry significant practical importance.

Oocyte meiosis represents a unique form of asymmetric cell division, wherein most of the maternal components are retained in the oocyte, resulting in the production of a highly polarized mature egg and a second polar body [11,12]. This asymmetric division is an intricately orchestrated cellular event of great importance in fertilization and initial embryonic development [13]. It requires the cytoskeleton, chromosomes, and an array of proteins to coordinate precisely within the oocyte to ensure accurate regulation [14]. The migration and positioning of the meiotic spindle at the cortex of the oocyte are crucial for asymmetric division, with actin microfilaments assuming a vital role in spindle migration [15,16]. As the meiotic spindle forms near the center of the cell, actin microfilaments accumulate around the periphery of the spindle and form actin flows, which facilitate spindle migration from the center to the cortex [17]. Actin filaments, initially evenly distributed in the oocyte cortex, become polarized during spindle migration. An actin cap forms near the spindle, covering the spindle area [18,19]. After the spindle has positioned at the cortex, cortical myosin and actin collaborate to form a contractile ring, which is instrumental in driving the asymmetric division of the oocyte [20,21]. Disruption of actin filaments retards chromosome movement towards the spindle poles and hinders the proper alignment of chromosomes during separation [22].

Sirtuins (Sirts), a family of evolutionarily conserved nicotinamide adenine dinucleotide (NAD^+)-dependent enzymes, including seven paralogs (Sirt1–7). These paralogs are defined by their unique terminal primary structures, which decide their varied subcellular localizations [23]. Among them, Sirt5 is localized within both the mitochondria and cytosol. Extensive proteomic studies have established that Sirt5 critically regulates lysine modifications, specifically malonylation, succinylation, and glutarylation [24]. Therefore, Sirt5 regulates cellular homeostasis, including critical metabolic pathways like fatty acid oxidation, the tricarboxylic acid cycle, glycolysis, and nitrogen metabolism, by modulating the expression and activity of various enzymes through post-translational modifications [25]. The involvement of Sirt5 in these diverse pathways suggests that its dysregulation may be linked to the development of various disorders, such as cardiovascular and neurodegenerative pathologies, infectious diseases, metabolic disorders, and cancers [26]. Despite these insights, the exact role of Sirt5 in cellular biology remains largely unclear. Emerging data suggest that sirtuins are involved in ovarian aging and oocyte maturation. For instance, Sirt3 expression decreases in an age-dependent manner in the ovary, and its deletion accelerates ovarian aging in mice. Furthermore, the abnormal function of Sirt3 contributes to the failure of oocyte meiotic maturation [27]. Additional sirtuin proteins, namely Sirt2 and Sirt4, exert noteworthy functions in oocyte meiotic maturation [28,29]. Although multiple studies have addressed the diverse roles of Sirt5 in various cellular processes, its specific role in orchestrating meiotic maturation in mouse oocytes and the underlying mechanisms remain largely unknown.

This study aims to explore the functions of Sirt5 during mouse oocyte meiotic maturation. Our findings reveal a notable decrease in Sirt5 protein levels in oocytes derived from aged mice. Significantly, we have identified previously uncharacterized roles of Sirt5 in spindle organization and actin-mediated spindle migration during the maturation of mouse oocytes.

Table 1
Primary antibody and application parameters.

Primary antibodies	Catalog number	Manufacturer	Dilution Rate	
			IF	WB
FITC-α-Tubulin	F2168	Sigma	1:200	/
SIRT5	ab105040	Abcam	1:100	1:500
Cofilin (phospho S3)	ab283500	Abcam	1:100	1:500
Profilin 1	ab124904	Abcam	1:100	1:500
N-WASP	ab126626	Abcam	1:100	1:500
HRP-conjugated GAPDH	AC035	ABclonal	/	1:2000
HRP-conjugated β-Actin	AC028	ABclonal	/	1:2000
Rhodamine Phalloidin	RM02835	ABclonal	1:500	/
HRP Goat Anti-Rabbit IgG (H + L)	AS014	ABclonal	/	1:5000
HRP Goat Anti-Mouse IgG (H + L)	AS003	ABclonal	/	1:5000

2. Materials and methods

2.1. Animals and ethics statement

Female Kunming (KM) mice (aged 3 weeks) were acquired from Jiangsu Huachuang Sino Pharmaceutical Technology Co., Ltd. (Taizhou, China), while female KM mice (aged 2 months and 12 months) were obtained from Vital River Laboratory Animal Technology Co., Ltd. (Beijing, China). These animals were accommodated at the Experimental Animal Center of Anhui Medical University under established conditions for mouse care and management. The protocols of this study were approved by the Animal Ethics Committee of Anhui Medical University (Approval number: LLSC20232146).

2.2. Antibody information

The antibodies utilized in this investigation, as well as their corresponding methods of application, are detailed in Table 1.

2.3. Oocyte collection and in vitro culture

Following euthanasia via cervical dislocation, the ovaries of the mice were surgically removed, incubated in DMEM/F12 (11320033, Gibco) supplemented with 50 μM 3-isobutyl-1-methylxanthine, and mechanically disrupted. A 100-mM stock solution of NRD167(CAS: 2166487-23-4, S9903, Selleck Chemicals), a selective Sirt5 inhibitor, was prepared in dimethyl sulfoxide (D8418, Sigma). Morphologically regular germinal vesicle-stage (GV-stage) oocytes were collected under a stereomicroscope (SMZ745, Nikon) and cultured in M16 medium (M7292, Sigma) containing 20, 40, or 60 μM of NRD167. and the control group contained an equal dose of DMSO solvent only. The oocytes were cultured in an environment of 5 % CO_2 and saturated humidity.

2.4. Immunofluorescence staining

Excised ovaries were fixed in 4 % paraformaldehyde for 24 h. This process was followed by a series of steps involving washing, dehydration, permeabilizing, embedding, and slicing to prepare tissue slides. The dewaxed tissue samples underwent antigen retrieval using ethylenediamine tetraacetic acid (P0085, Beyotime). Non-specific antigens in the samples were blocked using 10 % donkey serum.

Post-culture, the oocytes were immobilized and permeabilized, followed by blocking with 2 % bovine serum albumin. The subsequent steps were common for both tissue samples and oocytes. The samples were probed overnight at 4 °C with primary antibodies in a controlled-humidity chamber. Next, the samples were thoroughly washed thrice using phosphate-buffered saline, after which a secondary antibody was introduced. The samples then underwent a 1-h incubation at 37 °C in a humidified chamber. After the washing step, the slides were prepared for observation through mounting in an anti-fade solution containing 4′6-diamidino-2-phenylindole (P0131, Beyotime). A confocal laser-scanning microscope (LSM 980 with Airyscan 2, ZEISS) and an upright fluorescence microscope (Axioscope A1, ZEISS) were employed for imaging. Fluorescence intensity was analyzed using ZEN 3.8 or ImageJ software.

2.5. Western blot

Total protein was extracted from granulosa cells and oocytes in the ovary or oocytes cultured *in vitro* (n = 200) using RIPA lysis buffer (P0013, Beyotime) supplemented with SDS-PAGE sample loading buffer (P0295, Beyotime). The protein samples were heat-denatured at 95 °C for 10 min, electrophoretically separated by sodium dodecyl sulfate-polyacrylamide gel electrophoresis, and transferred to polyvinylidene difluoride membranes (IPVH00010, Millipore) with 0.45-μm pores. The membranes underwent a blocking phase in 5 % bovine serum albumin for 2 h and a washing process, followed by an incubation with the primary antibodies. Following another wash, the membrane underwent a 2-h incubation at an ambient temperature with secondary antibodies the next day. The detection and densitometric evaluation of the immunoblots was performed using a chemiluminescence detection kit (P0018, Beyotime), and the bands were visually documented using the Tanon 5200 image-capturing system (Tanon).

2.6. Real-time quantitative PCR

Total RNA was extracted using the RNAprep Pure Tissue Kit (DP431, TIANGEN). The primary steps involved lysing the tissue, washing, purification, and dissolving RNA, followed by purity analysis. A ratio of optical densities at 260 nm and 280 nm between 1.8 and 2.1 indicated good-quality RNA. The synthesis of cDNA was accomplished utilizing the PrimeScript™ RT Reagent Kit-Perfect Real Time (RR037, Takara). A 20-μL reaction mixture was prepared for quantitative PCR of the target gene, consisting of 7 μL of diethyl pyrocarbonate-treated water, 1 μL of cDNA, 2 μL of primers, and 10 μL of LightCycler 480 SYBR Green I Master (04707516001, Roche). The reaction was performed on the LightCycler® 96 system (Roche), with *GAPDH* serving as the internal control. The relative expression levels of the target gene were determined through the $2^{-\Delta\Delta CT}$ quantitative method. The sequence of the target gene was obtained from the NCBI database, and the primers were designed using PrimerBank. The primer sequences were as follows: Sirt5-Forward (F): 5′-CCAGTTGTGTTGTAGACGAAAGC-3′, Sirt5-Reverse (R): 5′-TTCCGAAAGTCTGCCATATTTGA-3′, Gapdh-F: 5′-AGGTCGGTGTGAACGGATTTG-3′, and Gapdh-R: 5′-GGGGTCGTTGATGGCAACA-3′.

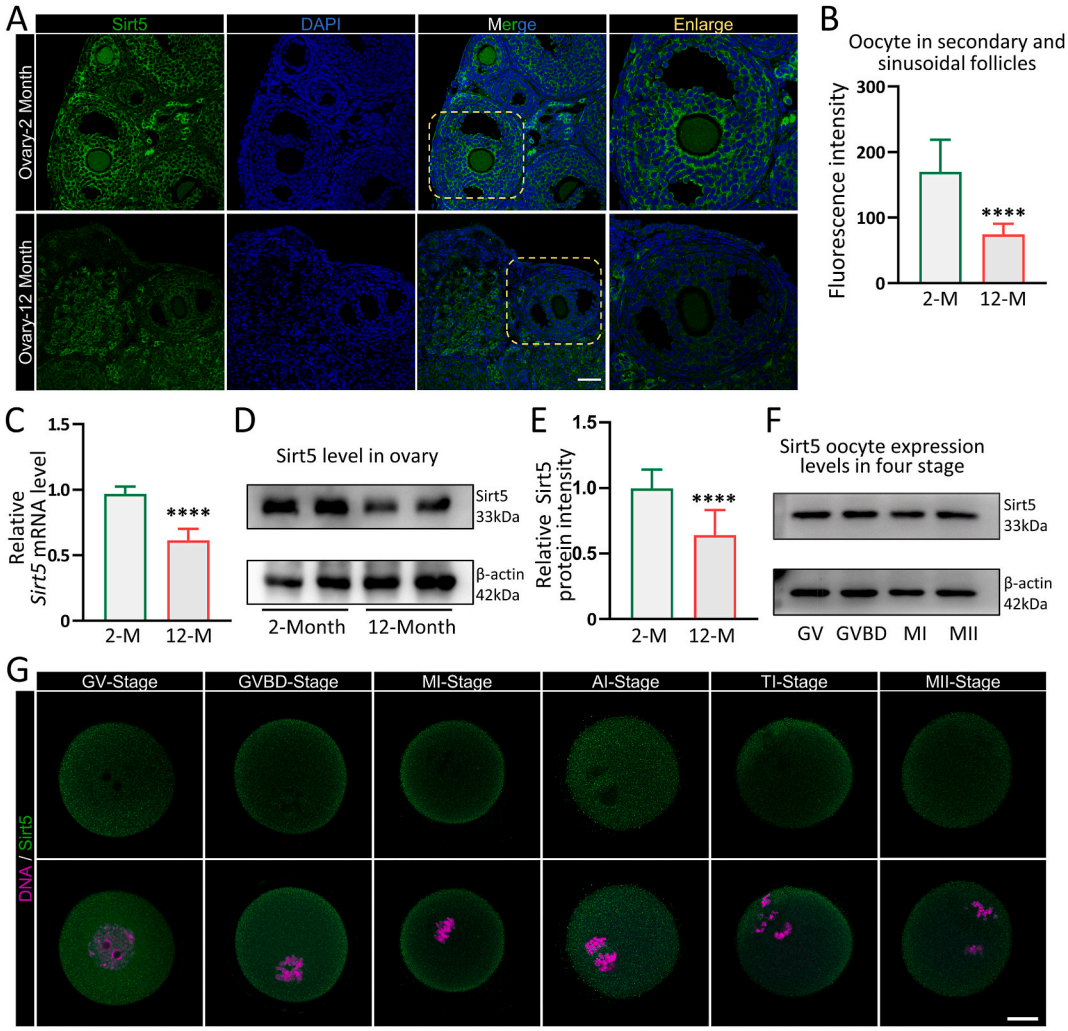

Fig. 1. Expression and localization of Sirt5 in mouse oocytes.
(A) Fluorescence images showing the expression of Sirt5 in young (2-month) and aged (12-month) ovaries. Green, Sirt5; Blue, nucleus; yellow dashed line is magnified area; scale bar = 20 μm. **(B)** Analysis of Sirt5 fluorescence intensity in secondary and sinusoidal follicles from young and aged ovaries (young, n = 35; aged, n = 15). ****, $p < 0.0001$. **(C)** Relative mRNA expression levels of Sirt5 in young and aged ovaries. ****, $p < 0.0001$. **(D)** Western blots of Sirt5 in young and aged ovaries. **(E)** Statistical analysis of relative protein expression levels of Sirt5 in young and aged ovaries. ****, $p < 0.0001$. **(F)** Expression of Sirt5 at different stages of oocyte development. **(G)** Fluorescence images depicting the localization of Sirt5 in oocytes at various developmental stages. GV, germinal vesicle; GVBD, germinal vesicle breakdown; MI, metaphase I; AI, anaphase I; TI, telophase I; MII, metaphase II. Green, Sirt5; Violet, nucleus; Scale bar = 20 μm.

2.7. Statistical analysis

A minimum of three independent experiments were conducted in this study. Data were represented as the mean ± standard deviation. Data were analyzed and plotted using GraphPad Prism 9. Statistical significance was evaluated using independent sample t-tests and analysis of variance. A p-value less than 0.05 was indicative of statistical significance.

3. Results

3.1. Expression and localization of Sirt5 in mouse oocytes

To examine the relationship between Sirt5 expression and oocyte quality, the ovaries of 2-month-old and 12-month-old female mice were subjected to immunofluorescence staining (Fig. 1A). Lack of undeveloped follicles (primordial and primary follicles) in aging ovaries, thus, the fluorescence intensity of Sirt5 in oocytes from secondary follicles and sinusoidal follicles was statistically analyzed. The fluorescence intensity of Sirt5 was markedly reduced in the oocytes of 12-month-old mice ovary (Fig. 1B). Sirt5 was

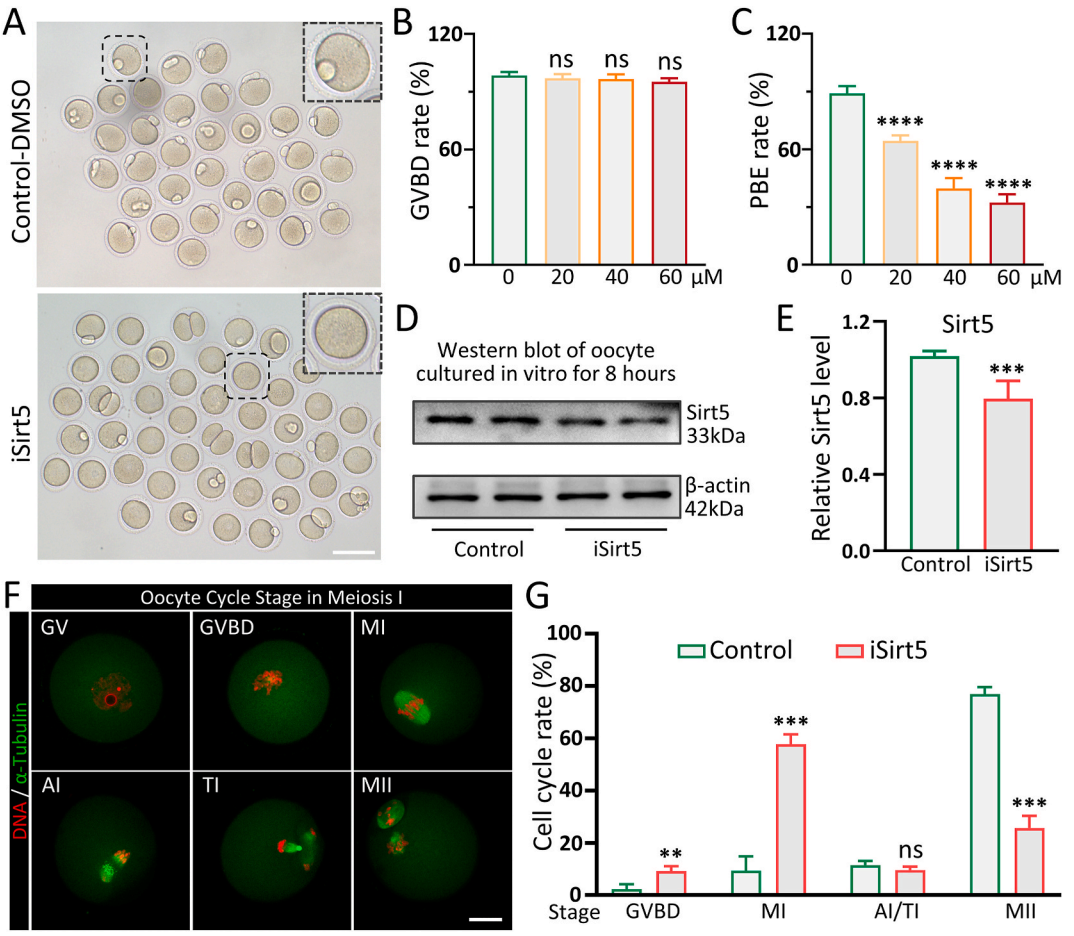

Fig. 2. Inhibition of Sirt5 leads to failure of oocyte meiotic maturation.
(A) Images of oocytes cultured *in vitro* for 14 h from two groups (Control and Sirt5 inhibitor-treated). Black dotted line indicates the magnified area. Scale bar = 100 μm. **(B)** Analysis of GVBD rates in oocytes cultured *in vitro* for 3 h in gradient concentrations of Sirt5 inhibitor (Control,n = 128; 20 μM, n = 128; 40 μM, n = 137; 60 μM, n = 127). ns, no significant. **(C)** Analysis of PBE rates in oocytes cultured for 14 h in gradient concentrations of Sirt5 inhibitor (Control,n = 128; 20 μM, n = 128; 40 μM, n = 137; 60 μM, n = 127). ****, $p < 0.0001$. **(D)** Western blots of oocytes from two groups cultured *in vitro* for 8 h. **(E)** Statistical analysis of the relative expression levels of Sirt5 in oocytes from two groups. ***, $p < 0.001$. **(F)** Representative fluorescence images of oocytes at major stages of the first meiotic division. Green, α-tubulin; Red, chromosomes. Scale bar = 20 μm. **(G)** Statistical analysis for cell cycle arrest of oocytes from both groups after 14 h of culture (Control, n = 95; iSirt5, n = 117). ns, no significant; **, $p < 0.01$; ***, $p < 0.001$; GV, germinal vesicle; GVBD, germinal vesicle breakdown; MI, metaphase I; AI, anaphase I; TI, telophase I; MII, metaphase II. PBE, polar body extrusion.

significantly downregulated at both the mRNA (Fig. 1C) and protein levels (Fig. 1D and E; Supplementary Fig. S2A) in the ovaries of 12-month-old mice. Subsequently, we examined the expression of Sirt5 at different stages of oocyte meiotic maturation to understand its role in mouse oocytes. Mouse oocytes were collected after 0, 3, 8, and 14 h of culture, representing the stages of GV, GV breakdown, metaphase I, and metaphase II. Western blot analysis revealed that Sirt5 was stably expressed throughout all the stages of meiotic division (Fig. 1F and Supplementary Fig. S2B). Subsequently, the localization of Sirt5 was evaluated during various stages of meiotic maturation in mouse oocytes, negative control excluded non-specific staining by Sirt5 antibodies (Supplementary Fig. S1). Immunofluorescence results indicated that Sirt5 was localized in both the cytoplasm and the nucleus during the GV stage but predominantly in the cytoplasm during the following stages (Fig. 1G). These findings suggest that Sirt5 may render notable effects on oocyte maturation and be involved in the age-related decline in oocyte quality.

3.2. Sirt5 inhibition leads to failure of oocyte meiotic maturation

This study proceeded to clarify the function of Sirt5 in mouse oocytes using the specific inhibitor NRD167 [30]. Sirt5 inhibition did not significantly affect the rate of GV breakdown after 3 h of culture (Fig. 2B), indicating that Sirt5 did not affect the resumption of meiosis. However, compared with control oocytes, Sirt5 inhibition markedly reduced the proportion of oocytes undergoing polar body extrusion (Fig. 2A and C). Western blot confirmed that treatment with NRD167 restricted the expression of Sirt5 (Fig. 2D and E;

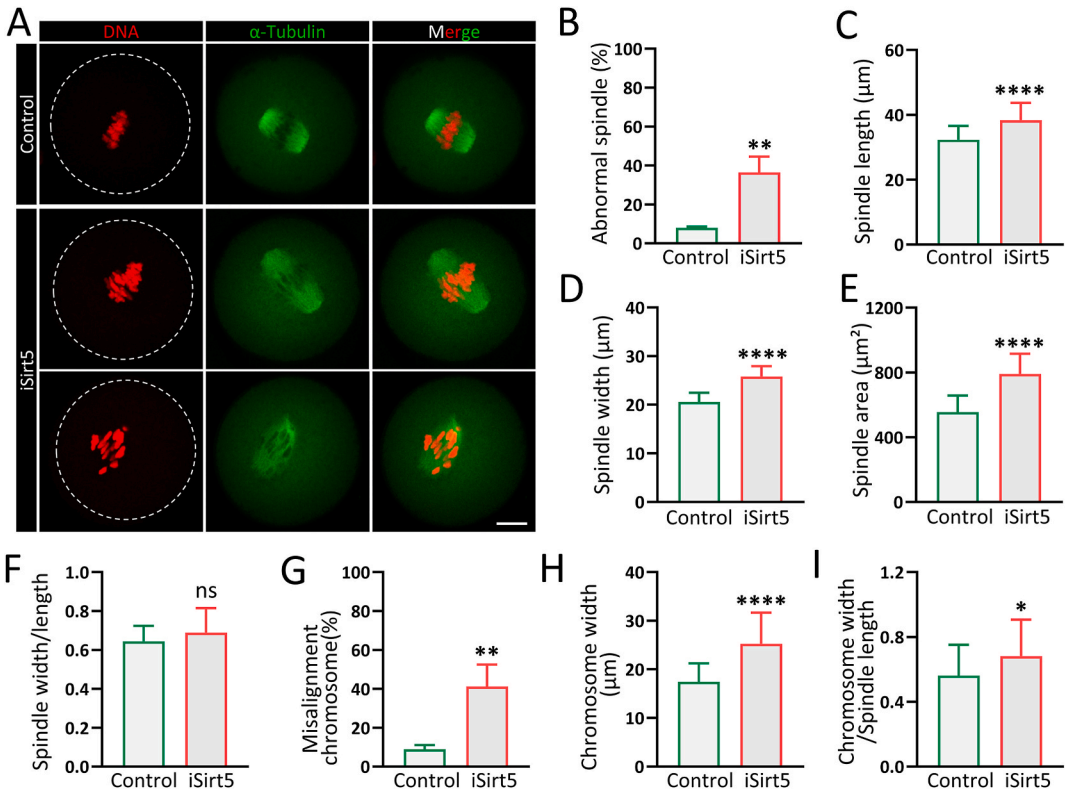

Fig. 3. Inhibition of Sirt5 causes abnormal spindle assembly and chromosome misalignment in oocytes.
(A) Immunofluorescence images of spindles and chromosomes in MI-stage (*in vitro* incubation for 8 h after release from prophase arrest) oocytes from two groups (Control and Sirt5 inhibitor-treated). Green, α-tubulin; Red, chromosomes. Scale bar = 20 μm. **(B)** Analysis of the proportion of abnormal spindles in MI-stage oocytes from both groups (Control, n = 108; iSirt5, n = 116). **, $p < 0.01$. **(C)** Analysis of spindle length in MI-stage oocytes from both groups (Control, n = 36; iSirt5, n = 42). ****, $p < 0.0001$. **(D)** Analysis of spindle width in MI-stage oocytes from both groups (Control, n = 36; iSirt5, n = 42). ****, $p < 0.0001$. **(E)** Analysis of spindle area in MI-stage oocytes from both groups (Control, n = 36; iSirt5, n = 42). ****, $p < 0.0001$. **(F)** Analysis of the ratio of spindle width to length in MI-stage oocytes from both groups (Control, n = 36; iSirt5, n = 42). ns, no significant. **(G)** Analysis of the proportion of MI-stage oocytes with abnormal chromosome alignment from both groups (Control, n = 108; iSirt5, n = 116). **, $p < 0.01$. **(H)** Analysis of chromosome width in MI-stage oocytes from both groups (Control, n = 36; iSirt5, n = 42). ****, $p < 0.0001$. **(I)** Analysis of the ratio of chromosome width to spindle length in MI-stage oocytes from both groups (Control, n = 36; iSirt5, n = 42). *, $p < 0.05$. MI, metaphase I.

Supplementary Fig. S2C). Subsequently, we examined the cell cycle entry of oocytes following Sirt5 inhibition. After 14 h of culture, most control oocytes had progressed to the metaphase II stage, whereas Sirt5-inhibited oocytes were arrested in the metaphase I stage (Fig. 2F and G). These findings implicate Sirt5 in the regulation of oocyte meiotic maturation.

3.3. Sirt5 inhibition causes abnormal spindle assembly and chromosome misalignment in oocytes

Proper spindle assembly is crucial for oocyte meiotic maturation. Given that Sirt5 inhibition induced oocyte arrest at the metaphase I stage, we evaluated the meiotic spindle morphology following Sirt5 inhibition. Control oocytes exhibited typical barrel-shaped spindles with accurately aligned chromosomes at the metaphase I stage (Fig. 3A). In contrast, Sirt5-inhibited oocytes displayed a prominently higher percentage of spindle abnormalities and severely misaligned chromosomes compared to the control group (Fig. 3A and B). Furthermore, percentage of chromosome misalignment, the length (Fig. 3C), width (Fig. 3D), and area (Fig. 3E) of spindles in Sirt5-inhibited oocytes were notably increased, although the ratio of spindle width to length (Fig. 3F) showed no significant difference. Concurrently, the percentage of chromosome misalignment (Fig. 3G), the chromosome width (Fig. 3H), and the ratio of chromosome width to spindle length (Fig. 3I)were markedly higher in Sirt5-inhibited oocytes than in control oocytes. These data indicate that Sirt5 inhibition notably disrupts spindle assembly and chromosome alignment in oocytes.

3.4. Sirt5 inhibition leads to failure of spindle migration

Intriguingly, the inhibition of Sirt5 led to defects in the asymmetric division of oocytes, resulting in the formation of abnormally large polar bodies (Fig. 4A). The rate of large polar body formation was significantly elevated in Sirt5-inhibited oocytes relative to

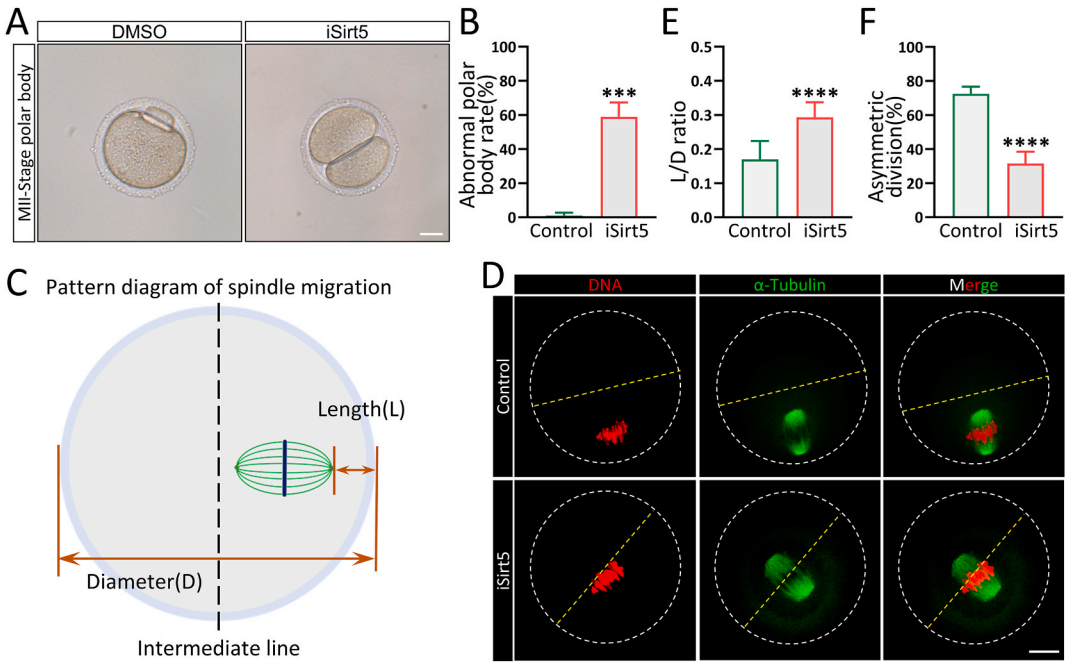

Fig. 4. Inhibition of Sirt5 leads to failure of spindle migration.
(A) Representative images of PBE in MII-stage oocytes from two groups (Control and Sirt5 inhibitor-treated). Scale bar = 20 μm. **(B)** Analysis of the proportion of abnormal large polar bodies in MII-stage oocytes from both groups (Control, n = 105; iSirt5, n = 109). ***, $p < 0.001$. **(C)** Schematic representation of spindle polar migration in MI-stage oocytes. Green, spindle; Blue, chromosomes. **(D)** Fluorescence images showing the location of the spindle in MI-stage (*in vitro* incubation for 8 h after release from prophase arrest) oocytes from both groups. The yellow dotted line indicates the median axis of the oocyte. Green, α-tubulin; Red, chromosomes. Scale bar = 20 μm. **(E)** Statistical analysis of the length-to-diameter ratio (L/D) in MI-stage oocytes from both groups (Control, n = 38; iSirt5, n = 44). ****, $p < 0.0001$. **(F)** Analysis of the proportion of MI-stage oocytes from both groups that completed polar spindle migration (Control, n = 119; iSirt5, n = 133). ****, $p < 0.0001$. MI, metaphase I; MII, metaphase II.

control oocytes (Fig. 4B). Spindle migration during oocyte maturation was critical for polar body formation (Fig. 4C). To investigate the mechanism underlying the formation of enlarged polar bodies, we studied the position of the spindle in metaphase I oocytes following Sirt5 inhibition. After 9 h of culture, most of the spindles in Sirt5-inhibited oocytes remained centrally located as compared to their cortical migration in control oocytes (Fig. 4D). To verify this observation, we quantified the distance from the spindle pole to the cortex (Length, L) relative to the diameter (D) of the oocyte (Fig. 4E), which allowed us to classify the spindles as either centrally or cortically positioned. The L/D ratio, indicative of spindle migration to the cortex, was substantially higher in Sirt5-inhibited oocytes compared with control oocytes (Fig. 4F). These observations reveal that Sirt5 mediates spindle migration, which is essential for the asymmetric division of oocytes.

3.5. *Sirt5 inhibition disrupts profilin–cofilin signaling-mediated actin dynamics*

Disruption of spindle migration hindered the formation of the actin cap, which is a critical feature of oocyte polarization. In the late metaphase I stage, control oocytes exhibited a prominent actin cap, while this structure was notably absent in the oocytes with Sirt5 inhibition (Fig. 5A). The quantitative assessment indicated a significant reduction in the percentage of oocytes with an actin cap in oocytes from the Sirt5-inhibited group relative to those in the control group (Fig. 5B). To delve deeper into the cause behind the spindle positioning defects, we analyzed the distribution of actin filaments following Sirt5 inhibition in the metaphase I stage. The results demonstrated that actin filament signals were notably elevated in Sirt5-inhibited oocytes (Fig. 5C–E). Statistical analysis indicated that the intensity of cytoplasmic actin fluorescence was markedly higher in Sirt5-inhibited oocytes compared with control oocytes (Fig. 5F). Similarly, cortical actin fluorescence intensity was significantly enhanced following Sirt5 inhibition (Fig. 5G). Thus, we focused on assessing the impact of Sirt5 on actin dynamics during oocyte meiosis.

Dynamic remodelling of the F-actin network in the cortex and cytoplasm is present during oocyte maturation. Profilin regulates actin polymerization, whereas Cofilin is an actin depolymerisation factor and together regulate actin dynamics remodelling. Interference with Profilin 1 and Cofilin function during oocyte maturation causes defects in spindle migration and polar body extrusion [31, 32]. Neural Wiskott–Aldrich syndrome protein (N-WASP) regulates the cortical cytoskeletal rearrangement, and N-WASP deletion impair midbody formation and second meiosis completion [33]. Western blot analysis indicated that the expression levels of profilin and phosphorylated cofilin were attenuated following Sirt5 inhibition (Fig. 5H, I and J; Supplementary Fig. S2D). However, the expression of N-WASP was unchanged after Sirt5 inhibition (Fig. 5H and K), suggesting that actin enhancement due to Sirt5 inhibition was not mediated by N-WASP-mediated actin assembly. These findings suggest that Sirt5 might influence the profilin–cofilin signaling

pathway for actin dynamics in mouse oocytes.

4. Discussion

Oocyte quality is an indicator of female reproductive health and is crucial for embryonic development and deciding the outcomes of pregnancy [1]. Upon achieving both nuclear and cytoplasmic maturation, fully developed oocytes attain the capacity for fertilization and can subsequently support embryonic growth [34]. Oocyte maturation is influenced by numerous intra- and extra-ovarian factors. In most mammals, the quality of oocytes declines with maternal age. Defects in oocyte meiosis can dramatically increase the incidence of infertility, miscarriages, and congenital anomalies [35]. Although numerous molecules and pathways have been proposed to counteract the age-associated defects in oocyte meiosis [36], the mechanistic underpinnings orchestrating meiosis still require detailed

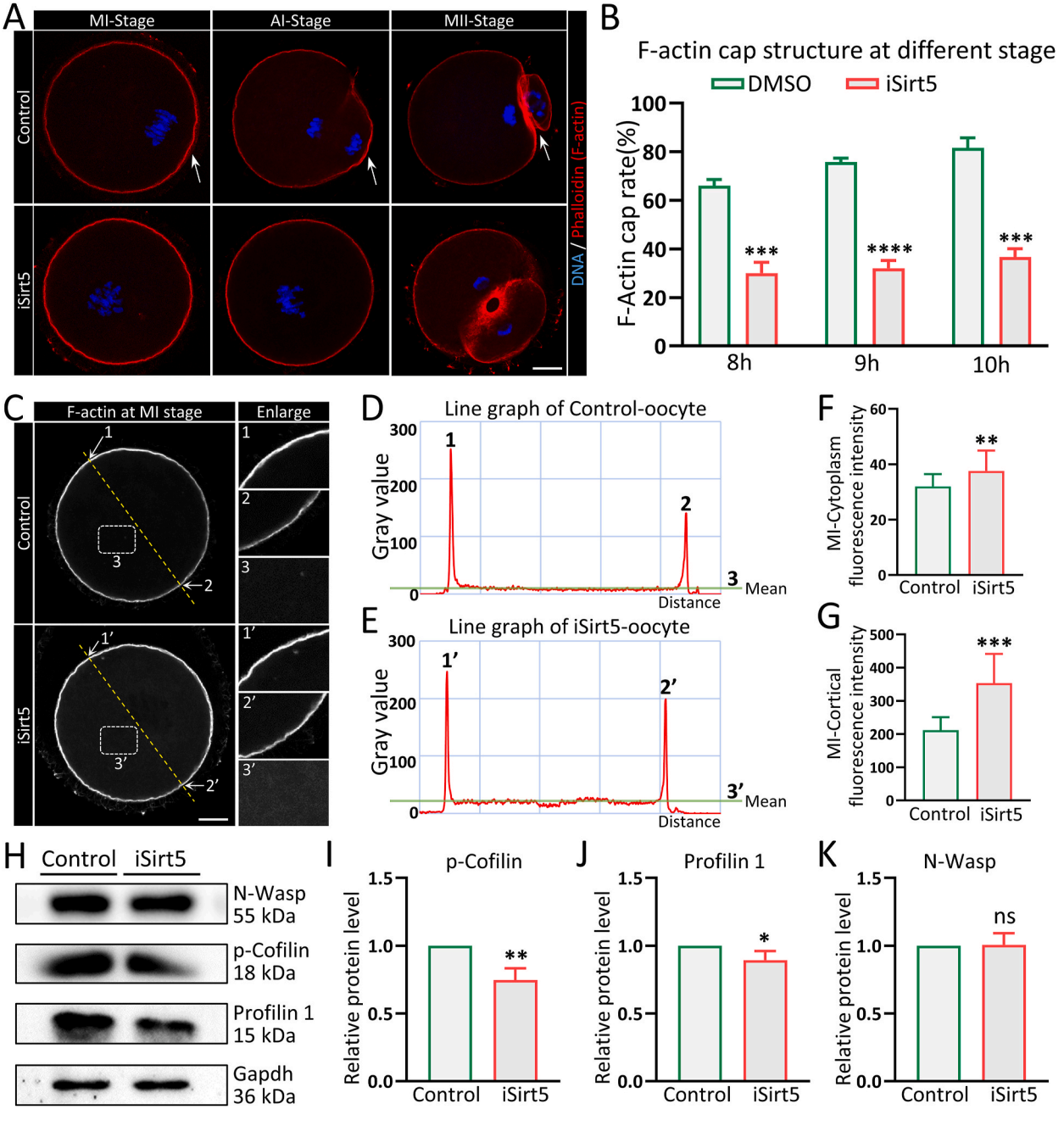

(caption on next page)

Fig. 5. Inhibition of Sirt5 disrupts profilin–cofilin signaling-mediated actin dynamics.
(A) Fluorescence images showing the distribution of F-actin in MI-stage (GVBD + 6 h), AI-stage (GVBD + 8 h) and MII-stage (GVBD + 10 h) oocytes from two groups (Control and Sirt5 inhibitor-treated). Phalloidin (Red) as a specific stain for F-actin. Bule, chromosomes. White arrow indicates F-actin cap structure. Scale bar = 20 μm. **(B)** Analysis of the proportion of oocytes forming F-actin cap structures after 8, 9, and 10 h of *in vitro* culture in both groups (8 h: Control, n = 86; iSirt5, n = 88; 9 h: Control, n = 82; iSirt5, n = 82; 10 h: Control, n = 94; iSirt5, n = 101). ***, $p < 0.001$; ****, $p < 0.0001$. **(C)** Distribution of F-actin in oocytes from both groups, with magnified views. Yellow dashed lines pass through cap structures and spindle areas. 1 and 2 indicate F-actin distribution on the cell membrane; 3 indicates F-actin distribution in the cytoplasm around the spindle. Scale bar = 20 μm. **(D)** Line graph of F-actin intensity in control group oocytes, with a green line indicating the average value of F-actin in the cytoplasm. **(E)** Line graph of F-actin intensity in Sirt5-inhibited oocytes, with a green line indicating the average value of F-actin in the cytoplasm. **(F)** Statistical analysis of cytoplasmic F-actin intensity in MI-Stage (GVBD + 6 h) oocytes from both groups (Control, n = 27; iSirt5, n = 24). **, $p < 0.01$. **(G)** Statistical analysis of cortical F-actin intensity in MI-Stage (GVBD + 6 h) oocytes from both groups (Control, n = 27; iSirt5, n = 24). ***, $p < 0.001$. **(H)** Western blots of N-Wasp, p-Cofilin, and Profilin 1 in oocytes cultured *in vitro* for 8 h from both groups. **(I)** Analysis of relative expression levels of p-cofilin in oocytes from both groups. **, $p < 0.01$. **(J)** Analysis of relative expression levels of profilin in oocytes from both groups. *, $p < 0.05$. **(K)** Analysis of relative expression levels of N-WASP in oocytes from both groups. ns, no significant. MI, metaphase I; AI, anaphase I; MII, metaphase II.

elucidation. In this study, we observed that Sirt5 expression was reduced in the oocytes of aging mice, suggesting a potential link between the age-associated decline in oocyte quality and Sirt5 expression. Consequently, we endeavored to investigate the role and mechanisms of Sirt5 in the meiotic maturation of mouse oocytes.

Our results demonstrated that Sirt5 was expressed at all stages of meiosis in mouse oocytes. To clarify the functional relevance of Sirt5 in oocyte meiosis, we utilized a specific Sirt5 inhibitor to diminish its activity. Sirt5 inhibition did not affect the resumption of meiosis but led to the failure of polar body extrusion. Further cell cycle entry analysis suggested that Sirt5 deficiency resulted in a decrease in the number of mature oocytes and a concurrent increase in the number of oocytes arrested at the metaphase I stage. These findings imply that Sirt5 confers a crucial regulatory role in oocyte meiosis.

Precise spindle assembly is pivotal for the correct segregation of chromosomes in meiosis and the generation of healthy oocytes [16]. Errors at any stage of spindle assembly and chromosomal alignment can lead to the production of aneuploid oocytes, which in turn may result in aneuploid embryos, causing embryo implantation failure and early pregnancy loss [8,9]. The fertilization of aneuploid human oocytes substantially contributes to pregnancy loss, and if the pregnancy proceeds to full term, it can result in developmental abnormalities. One of the reasons for the decline in oocyte quality in older women is the increasing prevalence of spindle and chromosomal defects with advancing maternal age [9,37,][38]]. Aberrant spindle formation and chromosome misalignment can activate the spindle assembly checkpoint, which halts cell cycle progression [39]. Therefore, to elucidate the causes of cell cycle arrest, we examined spindle morphology and chromosome alignment. Sirt5 inhibition led to spindle malformation and abnormal chromosome alignment. Therefore, the downregulation of Sirt5 may contribute to the decline in oocyte quality in older women.

In female animals, oocytes undergo asymmetric cytokinesis, producing a smaller first polar body and a larger oocyte that retains as much maternal material and energy as possible for early embryonic development [40]. We observed an interesting phenomenon in this study: Sirt5 inhibition not only prevented the release of the first polar body, but also resulted in the formation of large polar bodies. Hence, we hypothesize that Sirt5 might be implicated in the asymmetric cytoplasmic division of oocytes. The highly asymmetric division of oocytes largely depends on oocyte polarization, which is governed by several mechanisms, including the migration and anchoring of spindles, coupled with cortical restructuring [41,42]. Spindle migration was disrupted in Sirt5-inhibited oocytes, characterized by the continuous central location of the spindle within the cytoplasm. Therefore, Sirt5 is a crucial regulatory factor in spindle migration and asymmetric division during the meiotic maturation of mouse oocytes.

In mammalian oocytes, actin is actively involved in the asymmetric positioning of the spindle and in cortical polarization. Additionally, it serves as the fundamental driver of spindle dynamics and is critical for the asymmetric division of oocytes [11,43]. Sirt5 inhibition impeded the formation of an actin cap within oocytes, while the amount of cytoplasmic actin increased, suggesting that microfilament function may be affected. Defects in the microfilament cytoskeleton could be another significant reason for the meiotic arrest of oocytes induced by Sirt5 inhibition. Following this, our investigation focused on delineating the regulatory influence of Sirt5 on the assembly of actin in oocytes. Profilin1, a small actin-binding protein, is implicated in the regulation of actin assembly [44]. In oocytes, profilin1 is located around the meiotic spindle and co-localizes with cytoplasmic actin, organizing the dynamic cytoplasmic actin network and mediating spindle migration towards the cortex [45]. Knockout of profilin1 leads to increased actin polymerization in both the cell membrane and cytoplasm [45]. We found that Sirt5 inhibition decreased profilin1 expression and increased actin fluorescence signals at the cell membrane and cytoplasm, suggesting that Profilin 1 is critically involved in the microfilament defects induced by Sirt5 inhibition. Effective disassembly of actin during oocyte maturation is crucial for asymmetric division [31,46]. The enhanced actin levels in the cell membrane and cytoplasm led us to speculate whether actin depolymerisation was also impaired following Sirt5 inhibition [31]. Cofilin is a member of the actin depolymerisation factor family with actin filament cleavage activity. And Regulation of Cofilin activity occurs primarily through inhibitory phosphorylation of Ser3 [31]. In addition, several studies have reported that reduced p-Cofilin is associated with spindle migration failure and symmetric division of oocytes [47,48]. We examined the expression of p-Cofilin. Sirt5 inhibition diminished the levels of phosphorylated Cofilin, while the expression of the actin nucleator nuclear Wiskott–Aldrich syndrome protein remained unchanged. Thus, Sirt5 regulates actin dynamics by affecting the level of the phosphorylated Cofilin and Profilin 1, subsequently controlling spindle migration and asymmetric cytokinesis. It is important to note that failure of spindle migration leads not only to unequal cytoplasmic division, but also to an inability of the cytoplasm to divide, and

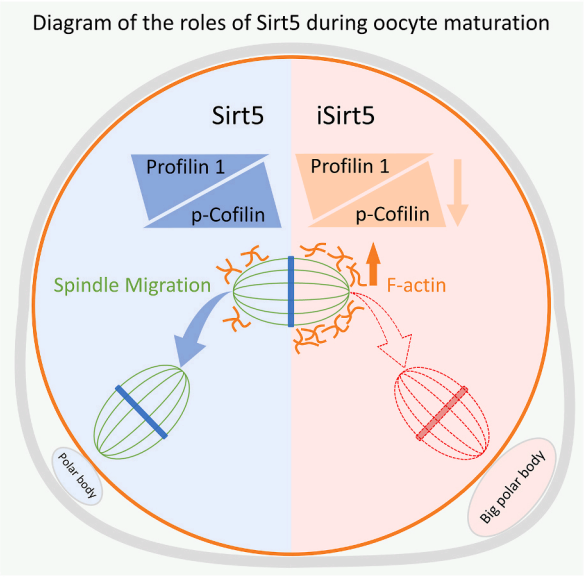

Fig. 6. Diagram of the roles of Sirt5 during oocyte maturation.
Profilin 1 and p-Cofilin are involved in the dynamic remodelling of the F-actin network in the cortex and cytoplasm during oocyte maturation. In vitro culture, inhibition of Sirt5 in oocytes causes disruption remodelling of F-actin in the cortex and cytoplasm, leading to defects in spindle migration and polar body extrusion.

ultimately to oocyte blockage during the MI stage.

In summary, our data suggest that Sirt5 inhibition during oocyte maturation disrupts actin dynamics by affecting the level of the phosphorylated Cofilin and Profilin 1, impairing spindle migration, which ultimately leads to equal division and maturation failure in oocytes (Fig. 6).

Funding information

This study was supported by National Key Research and Development Program of China (2022YFC2703000), Anhui Key Research and Development Program (No. 202204295107020041) and Postgraduate Innovation Research and Practice Program of Anhui Medical University (No. YJS20230029).

Ethical approval

For animal experiments, the protocols of this study were approved by the Animal Ethics Committee of Anhui Medical University (Approval number: LLSC20232146).

Data availability statement

The experimental study data are available upon request.

CRediT authorship contribution statement

Cong Ma: Writing – original draft, Visualization, Methodology, Funding acquisition, Formal analysis, Data curation, Conceptualization. **Xueke Zhang:** Visualization, Validation, Resources, Formal analysis, Data curation. **Yingying Zhang:** Visualization, Validation, Resources. **Hongzhen Ruan:** Validation, Formal analysis, Data curation. **Xiaofeng Xu:** Investigation, Funding acquisition. **Caiyun Wu:** Writing – review & editing. **Zhiming Ding:** Writing – review & editing, Validation, Supervision, Project administration, Funding acquisition, Conceptualization. **Yunxia Cao:** Writing – review & editing, Supervision, Project administration, Funding acquisition, Conceptualization.

Declaration of competing interest

The authors declare that they have no known competing financial interests or personal relationships that could have appeared to influence the work reported in this paper.

Acknowledgements

We are grateful for the financial support from the National Funding Committee, and respect for experimental animals.

Appendix A. Supplementary data

Supplementary data to this article can be found online at https://doi.org/10.1016/j.heliyon.2024.e32466.

References

[1] E.E. Telfer, J. Grosbois, Y.L. Odey, R. Rosario, R.A. Anderson, Making a good egg: human oocyte health, aging, and in vitro development, Physiol. Rev. 103 (2023) 2623–2677.
[2] F.J. Broekmans, M.R. Soules, B.C. Fauser, Ovarian aging: mechanisms and clinical consequences, Endocr. Rev. 30 (2009) 465–493.
[3] Y. Qin, Y. Choi, H. Zhao, J.L. Simpson, Z.J. Chen, A. Rajkovic, NOBOX homeobox mutation causes premature ovarian failure, Am. J. Hum. Genet. 81 (2007) 576–581.
[4] X. Guo, Y. Zhu, L. Guo, Y. Qi, X. Liu, J. Wang, J. Zhang, L. Cui, Y. Shi, Q. Wang, C. Liu, G. Lu, Y. Liu, T. Li, S. Hong, Y. Qin, X. Xiong, H. Wu, L. Huang, H. Huang, C. Gu, B. Li, J. Li, BCAA insufficiency leads to premature ovarian insufficiency via ceramide-induced elevation of ROS, EMBO Mol. Med. 15 (2023) e17450.
[5] A. Haavisto, L. Wettergren, C. Lampic, P.M. Lähteenmäki, K. Jahnukainen, Premature ovarian insufficiency and chance of pregnancy after childhood cancer: a population-based study (the Fex-Can study), Int. J. Cancer 153 (2023) 644–653.
[6] D. Keefe, M. Kumar, K. Kalmbach, Oocyte competency is the key to embryo potential, Fertil. Steril. 103 (2015) 317–322.
[7] M. MacLennan, J.H. Crichton, C.J. Playfoot, I.R. Adams, Oocyte development, meiosis and aneuploidy, Semin. Cell Dev. Biol. 45 (2015) 68–76.
[8] M. Mikwar, A.J. MacFarlane, F. Marchetti, Mechanisms of oocyte aneuploidy associated with advanced maternal age, Mutation research, Reviews in mutation research 785 (2020) 108320.
[9] C. Charalambous, A. Webster, M. Schuh, Aneuploidy in mammalian oocytes and the impact of maternal ageing, Nat. Rev. Mol. Cell Biol. 24 (2023) 27–44.
[10] M. Vallet-Buisan, R. Mecca, C. Jones, K. Coward, M. Yeste, Contribution of semen to early embryo development: fertilization and beyond, Hum. Reprod. Update 29 (2023) 395–433.
[11] X. Duan, S.C. Sun, Actin cytoskeleton dynamics in mammalian oocyte meiosis, Biol. Reprod. 100 (2019) 15–24.
[12] S. Pfender, V. Kuznetsov, S. Pleiser, E. Kerkhoff, M. Schuh, Spire-type actin nucleators cooperate with Formin-2 to drive asymmetric oocyte division, Curr. Biol. 21 (2011) 955–960.
[13] B. Xie, L. Zhang, H. Zhao, Q. Bai, Y. Fan, X. Zhu, Y. Yu, R. Li, X. Liang, Q.Y. Sun, M. Li, J. Qiao, Poly(ADP-ribose) mediates asymmetric division of mouse oocyte, Cell Res. 28 (2018) 462–475.
[14] B. Mogessie, K. Scheffler, M. Schuh, Assembly and positioning of the oocyte meiotic spindle, Annu. Rev. Cell Dev. Biol. 34 (2018) 381–403.
[15] K.H. Siller, C.Q. Doe, Spindle orientation during asymmetric cell division, Nat. Cell Biol. 11 (2009) 365–374.
[16] J.N. Kincade, A. Hlavacek, T. Akera, A.Z. Balboula, Initial spindle positioning at the oocyte center protects against incorrect kinetochore-microtubule attachment and aneuploidy in mice, Sci. Adv. 9 (2023) eadd7397.
[17] Y.T. He, L.L. Yang, S.M. Luo, W. Shen, S. Yin, Q.Y. Sun, PAK4 regulates actin and microtubule dynamics during meiotic maturation in mouse oocyte, Int. J. Biol. Sci. 15 (2019) 2408–2418.
[18] B. Maro, M.H. Johnson, S.J. Pickering, G. Flach, Changes in actin distribution during fertilization of the mouse egg, J. Embryol. Exp. Morphol. 81 (1984) 211–237.
[19] L.L. Hu, M.H. Pan, F.L. Yang, Z.A. Zong, F. Tang, Z.N. Pan, X. Lu, Y.P. Ren, J.L. Wang, S.C. Sun, FASCIN regulates actin assembly for spindle movement and polar body extrusion in mouse oocyte meiosis, J. Cell. Physiol. 236 (2021) 7725–7733.
[20] W.S. Yuen, Q.H. Zhang, A. Bourdais, D. Adhikari, G. Halet, J. Carroll, Polo-like kinase 1 promotes Cdc42-induced actin polymerization for asymmetric division in oocytes, Open biology 13 (2023) 220326.
[21] A. Bourdais, B. Dehapiot, G. Halet, MRCK activates mouse oocyte myosin II for spindle rotation and male pronucleus centration, J. Cell Biol. 222 (2023).
[22] Y.J. Jo, W.I. Jang, S. Namgoong, N.H. Kim, Actin-capping proteins play essential roles in the asymmetric division of maturing mouse oocytes, J. Cell Sci. 128 (2015) 160–170.
[23] C. Tatone, G. Di Emidio, A. Barbonetti, G. Carta, A.M. Luciano, S. Falone, F. Amicarelli, Sirtuins in gamete biology and reproductive physiology: emerging roles and therapeutic potential in female and male infertility, Hum. Reprod. Update 24 (2018) 267–289.
[24] M.J. Rardin, W. He, Y. Nishida, J.C. Newman, C. Carrico, S.R. Danielson, A. Guo, P. Gut, A.K. Sahu, B. Li, R. Uppala, M. Fitch, T. Riiff, L. Zhu, J. Zhou, D. Mulhern, R.D. Stevens, O.R. Ilkayeva, C.B. Newgard, M.P. Jacobson, M. Hellerstein, E.S. Goetzman, B.W. Gibson, E. Verdin, SIRT5 regulates the mitochondrial lysine succinylome and metabolic networks, Cell Metabol. 18 (2013) 920–933.
[25] J. Park, Y. Chen, D.X. Tishkoff, C. Peng, M. Tan, L. Dai, Z. Xie, Y. Zhang, B.M. Zwaans, M.E. Skinner, D.B. Lombard, Y. Zhao, SIRT5-mediated lysine desuccinylation impacts diverse metabolic pathways, Mol. Cell 50 (2013) 919–930.
[26] Z. Ji, G.H. Liu, J. Qu, Mitochondrial sirtuins, metabolism, and aging, Journal of genetics and genomics = Yi chuan xue bao 49 (2022) 287–298.
[27] Q. Yang, Y. Wang, H. Wang, H. Li, J. Zhu, L. Cong, J. Xu, W. Chen, Y. Jiang, Y. Sun, NAD(+) repletion attenuates obesity-induced oocyte mitochondrial dysfunction and offspring metabolic abnormalities via a SIRT3-dependent pathway, Clin. Transl. Med. 11 (2021) e628.
[28] L. Zhang, X. Hou, R. Ma, K. Moley, T. Schedl, Q. Wang, Sirt2 functions in spindle organization and chromosome alignment in mouse oocyte meiosis, Faseb. J. : official publication of the Federation of American Societies for Experimental Biology 28 (2014) 1435–1445.
[29] J. Zeng, M. Jiang, X. Wu, F. Diao, D. Qiu, X. Hou, H. Wang, L. Li, C. Li, J. Ge, J. Liu, X. Ou, Q. Wang, SIRT4 is essential for metabolic control and meiotic structure during mouse oocyte maturation, Aging Cell 17 (2018) e12789.
[30] D. Yan, A. Franzini, A.D. Pomicter, B.J. Halverson, O. Antelope, C.C. Mason, J.M. Ahmann, A.V. Senina, N.A. Vellore, C.L. Jones, M.S. Zabriskie, H. Than, M. J. Xiao, A. van Scoyk, A.B. Patel, P.M. Clair, W.L. Heaton, S.C. Owen, J.L. Andersen, C.M. Egbert, J.A. Reisz, A. D'Alessandro, J.E. Cox, K.C. Gantz, H. M. Redwine, S.M. Iyer, J.S. Khorashad, N. Rajabi, C.A. Olsen, T. O'Hare, M.W. Deininger, SIRT5 IS A druggable metabolic vulnerability in acute myeloid leukemia, Blood cancer discovery 2 (2021) 266–287.
[31] A. Bourdais, B. Dehapiot, G. Halet, Cofilin regulates actin network homeostasis and microvilli length in mouse oocytes, J. Cell Sci. 134 (2021).
[32] V.Y. Rawe, C. Payne, G. Schatten, Profilin and actin-related proteins regulate microfilament dynamics during early mammalian embryogenesis, Human reproduction (Oxford, England) 21 (2006) 1143–1153.
[33] Z.B. Wang, X.S. Ma, M.W. Hu, Z.Z. Jiang, T.G. Meng, M.Z. Dong, L.H. Fan, Y.C. Ouyang, S.B. Snapper, H. Schatten, Q.Y. Sun, Oocyte-specific deletion of N-WASP does not affect oocyte polarity, but causes failure of meiosis II completion, Mol. Hum. Reprod. 22 (2016) 613–621.
[34] G. Coticchio, M. Dal Canto, M. Mignini Renzini, M.C. Guglielmo, F. Brambillasca, D. Turchi, P.V. Novara, R. Fadini, Oocyte maturation: gamete-somatic cells interactions, meiotic resumption, cytoskeletal dynamics and cytoplasmic reorganization, Hum. Reprod. Update 21 (2015) 427–454.
[35] J. van der Reest, G. Nardini Cecchino, M.C. Haigis, P. Kordowitzki, Mitochondria: their relevance during oocyte ageing, Ageing Res. Rev. 70 (2021) 101378.
[36] P. Kordowitzki, S. Graczyk, A. Haghani, M. Klutstein, Oocyte aging: a multifactorial phenomenon in A unique cell, Aging and disease (2023).

[37] J. Dong, L. Jin, S. Bao, B. Chen, Y. Zeng, Y. Luo, X. Du, Q. Sang, T. Wu, L. Wang, Ectopic expression of human TUBB8 leads to increased aneuploidy in mouse oocytes, Cell discovery 9 (2023) 105.
[38] B. Mogessie, Advances and surprises in a decade of oocyte meiosis research, Essays Biochem. 64 (2020) 263–275.
[39] P. Lara-Gonzalez, F.G. Westhorpe, S.S. Taylor, The spindle assembly checkpoint, Curr. Biol. 22 (2012) R966–R980.
[40] G.I. Jung, D. Londoño-Vásquez, S. Park, A.R. Skop, A.Z. Balboula, K. Schindler, An oocyte meiotic midbody cap is required for developmental competence in mice, Nat. Commun. 14 (2023) 7419.
[41] B. Dehapiot, R. Clément, A. Bourdais, V. Carrière, S. Huet, G. Halet, RhoA- and Cdc42-induced antagonistic forces underlie symmetry breaking and spindle rotation in mouse oocytes, PLoS Biol. 19 (2021) e3001376.
[42] Z.L. Jin, X.R. Yao, L. Wen, G. Hao, J.W. Kwon, J. Hao, N.H. Kim, AIP1 and Cofilin control the actin dynamics to modulate the asymmetric division and cytokinesis in mouse oocytes, Faseb. J. : official publication of the Federation of American Societies for Experimental Biology 34 (2020) 11292–11306.
[43] Z. Holubcová, G. Howard, M. Schuh, Vesicles modulate an actin network for asymmetric spindle positioning, Nat. Cell Biol. 15 (2013) 937–947.
[44] J.D. Rotty, C. Wu, E.M. Haynes, C. Suarez, J.D. Winkelman, H.E. Johnson, J.M. Haugh, D.R. Kovar, J.E. Bear, Profilin-1 serves as a gatekeeper for actin assembly by Arp2/3-dependent and -independent pathways, Dev. Cell 32 (2015) 54–67.
[45] J. Liu, Q.C. Wang, X. Duan, X.S. Cui, N.H. Kim, Y. Zhang, S.C. Sun, Profilin 1 plays feedback role in actin-mediated polar body extrusion in mouse oocytes, Reprod. Fertil. Dev. 30 (2018) 752–758.
[46] J. Azoury, K.W. Lee, V. Georget, P. Hikal, M.H. Verlhac, Symmetry breaking in mouse oocytes requires transient F-actin meshwork destabilization, Development 138 (2011) 2903–2908.
[47] Z.N. Pan, J.C. Liu, J.Q. Ju, Y. Wang, S.C. Sun, LRRK2 regulates actin assembly for spindle migration and mitochondrial function in mouse oocyte meiosis, J. Mol. Cell Biol. 14 (2022).
[48] Y. Zhang, X. Wan, H.H. Wang, M.H. Pan, Z.N. Pan, S.C. Sun, RAB35 depletion affects spindle formation and actin-based spindle migration in mouse oocyte meiosis, Mol. Hum. Reprod. 25 (2019) 359–372.